Scattering from a Cylindrical Waveguide with Rectangular Corrugations

Haeng S. Lee and Hyo J. Eom, *Senior Member, IEEE*

***Abstract*—Electromagnetic scattering from a circular cylindrical waveguide with rectangular corrugations is considered in this paper. An analysis method based on dyadic Green's functions and Fourier transforms is used to get the field in terms of modal currents induced on the corrugation openings. The fields are expressed through a series of modal eigenfunctions in the corrugations, and are integrated to get the unknown expansion coefficients. This analysis method can easily be extended to find the dispersion relations of the corrugated waveguide. The series solution obtained is analytic and suitable for numerical computation. Numerical results are presented to illustrate the scattering behavior of a corrugated cylindrical waveguide in terms of frequency and waveguide geometry.**

***Index Terms*—Corrugated waveguide, dyadic Green function, mode converter.**

I. Introduction

RADIATION from the open end of a corrugated hybrid-mode circular waveguide has excellent properties, such as low sidelobes, cross-polarization levels, axial beam symmetry, and low attenuation. Such properties cannot be obtained by a smooth-walled circular cylinder. To put it simply, circumferential slots enable the support of both TE and TM modes with the same propagation wavenumber to get improved quality mode characteristics [1]. With this basic idea, analysis methods based on anisotropic surface impedances in the corrugated waveguide have been used with sufficient accuracy when the corrugation widths are small compared to the wavelength at operating frequencies [2]. When the corrugation width is comparable to the wavelength, this method based on simple theory fails, and another technique based on a modal expansion method has been used [3]. In some approaches, the corrugated waveguides are analyzed with the assumption that they are made of infinite series of junctions of two smooth walled cylinders with different radii, and can be solved by cascading as many scattering matrices as the number of corrugations [4], [5]. Although these methods are simple to use and helpful in understanding the scattering mechanism, they consume many computational resources during the calculations of matrix equations, which often are of high dimensions.

Manuscript received August 20, 1999. This work was supported by the Korea Science and Engineering Foundation Interdisciplinary Research Program under Grant 1999-1-302-011-3.

H. S. Lee was with the Department of Electrical Engineering, Korea Advanced Institute of Science and Technology, 373-1 Taejon, Korea. He is now with the LCT Electronics Institute of Technology, 373-1 Taejon, Korea.

H. J. Eom is with the Department of Electrical Engineering, Korea Advanced Institute of Science and Technology, 373-1 Taejon, Korea (e-mail: hjeom@ee.kaist.ac.kr).

Publisher Item Identifier S 0018-9480(01)01071-7.

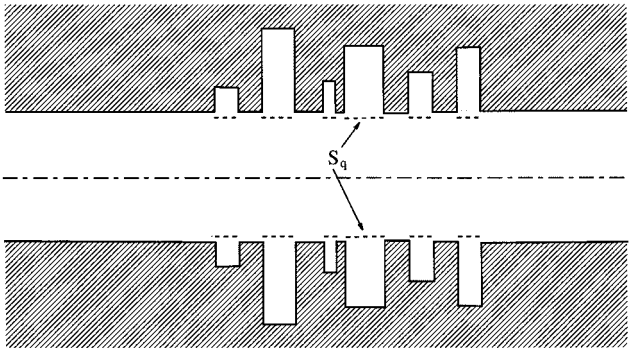

Fig. 1. S_q is the surface area at the opening of the qth corrugation ($S_\Sigma = \sum_p S_p$).

As shown in the following sections, our method solves the problem using lower dimension matrix equations. This is due to expressing the field in the waveguide with integrals of equivalent magnetic modal currents. Da Silva [5] has adopted the concept of an equivalent magnetic current in the analysis, but use the equivalent currents in obtaining a single scattering matrix, thus limiting applicability. In our method, modal currents in each corrugation are integrated to get field expressions in the guide and enable us to analyze the waveguide with nonuniform aperiodic corrugations.

In this paper, scattering analysis of the circular to corrugated waveguide junctions are treated with the modal equivalent magnetic currents method, and then application to a mode converter is considered. Although derivations are given for the cases with a finite number of corrugations, the analysis can be extended to the case with an infinite number of corrugations. In the Appendix, we show the extension to the infinite case and present characteristic equations that are used to find dispersion relations. The method used in this paper enable us to get a series solution for the modal currents that is rapidly convergent and numerically efficient.

II. Analysis Method

In this section, we show that fields in a waveguide with arbitrarily shaped corrugations can be obtained if only the fields at the opening of the corrugations are known (see Fig. 1). We assume that the geometry of the problem comprises a region of a cylinder and that of corrugations. The fields in the cylinder are represented as follows:

$$\overline{E} = \int_{-\infty}^{\infty} \tilde{\pi}_m(\zeta)\overline{e}_m(\zeta, \overline{x})\, d\zeta + \int_{-\infty}^{\infty} \tilde{\pi}_e(\zeta)\overline{e}_e(\zeta, \overline{x})\, d\zeta \quad (1)$$

$$\overline{H} = \int_{-\infty}^{\infty} \tilde{\pi}_m(\zeta)\overline{h}_m(\zeta, \overline{x})\, d\zeta + \int_{-\infty}^{\infty} \tilde{\pi}_e(\zeta)\overline{h}_e(\zeta, \overline{x})\, d\zeta \quad (2)$$

where $\overline{e}, \overline{h}$ are electric and magnetic eigenfunctions with eigenvalue ζ, subscripts m and e stand for TM and TE modes, and $\overline{x}$ is the position vector. We use a continuous spectrum representation to satisfy the boundary conditions imposed on the inner surface of the corrugated waveguide, which extends from $-\infty$ to $+\infty$.

The expansion coefficients $\tilde{\pi}_m(\zeta)$ and $\tilde{\pi}_e(\zeta)$ can be found using the orthogonality properties of the eigenfunctions. We assume that appropriate normalizations are made. Multiplying the electric-field equation above by $\overline{h}_m$ and integrating over the cylinder surface

$$\begin{aligned}\int_S \overline{E}(\overline{x}')\times\overline{h}_m^*(\zeta,\overline{x}')\cdot d\overline{a}' &= \int_{-\infty}^{\infty}\tilde{\pi}_m(\zeta')\underbrace{\int_S \overline{e}_m(\zeta',\overline{x}')\times\overline{h}_m^*(\zeta,\overline{x}')\cdot d\overline{a}'}_{\delta(\zeta-\zeta')}\,d\zeta' \\ &= \tilde{\pi}_m(\zeta). \end{aligned} \tag{3}$$

Therefore,

$$\begin{aligned}\overline{E}_m &= \int_{-\infty}^{\infty}\left[\int_S \overline{E}(\overline{x}')\times\overline{h}_m^*(\zeta,\overline{x}')\cdot d\overline{a}'\right]\overline{e}_m(\zeta,\overline{x})\,d\zeta \\ &= \int_{S_\Sigma}[d\overline{a}'\times\overline{E}(\overline{x}')]\cdot\int_{-\infty}^{\infty}\overline{h}_m^*(\zeta,\overline{x}')\overline{e}_m(\zeta,\overline{x})\,d\zeta \\ &= \int_{S_\Sigma}\overline{J}(\overline{x}')\cdot\overline{\overline{G}}_m(\overline{x},\overline{x}')\,da' \end{aligned} \tag{4}$$

where $\overline{J}(\overline{x}) = \hat{n}\times\overline{E}(\overline{x})$ is the equivalent magnetic current and $\overline{\overline{G}}_m(\overline{x},\overline{x}') = \int_{-\infty}^{\infty}\overline{h}_m^*(\zeta,\overline{x}')\overline{e}_m(\zeta,\overline{x})\,d\zeta$ is the TM-mode dyadic Green's function.

In a like manner, $\tilde{\pi}_e(\zeta)$ is to be found, and the TE electric fields are as follows:

$$\overline{E}_e = \int_{S_\Sigma}\overline{J}(\overline{x}')\cdot\overline{\overline{G}}_e(\overline{x},\overline{x}')\,da' \tag{5}$$

where $\overline{\overline{G}}_e(\overline{x},\overline{x}') = \int_{-\infty}^{\infty}\overline{h}_e^*(\zeta,\overline{x}')\overline{e}_e(\zeta,\overline{x})\,d\zeta$ is the TE mode dyadic Green's function.

The total electric field in the cylindrical region is

$$\overline{E} = \overline{E}_m + \overline{E}_e = \int_{S_\Sigma}\overline{J}(\overline{x}')\cdot\overline{\overline{G}}(\overline{x},\overline{x}')\,da' \tag{6}$$

where $\overline{\overline{G}}(\overline{x},\overline{x}') = \overline{\overline{G}}_m(\overline{x},\overline{x}')+\overline{\overline{G}}_e(\overline{x},\overline{x}')$. The fields are represented as a surface integral of the transverse fields at the opening of the corrugations.

Although we have derived integral equations based on the dyadic Green's functions, the expressions still have an unknown equivalent current at the opening of each corrugation. To solve the problem, we expand the fields in the corrugations as a sum of discrete eigenfunctions with unknown coefficients. We then find the unknown coefficients using the magnetic-field continuity.

Multiplying the original magnetic-field equation by discrete eigenfunctions ($\overline{e}_m^{d*}$ or $\overline{e}_e^{d*}$) and integrating as before, we get the final equations relating the unknown coefficients

$$\begin{aligned}&\int_{S_q}\overline{e}_m^{d*}(\overline{x})\times\overline{H}(\overline{x})\cdot d\overline{a} \\ &\quad= \int_{S_\Sigma}\int_{S_q}\overline{J}(\overline{x}')\cdot\overline{\overline{K}}(\overline{x},\overline{x}')\cdot\overline{J}_m^{d*}(\overline{x})\,da\,da' \end{aligned} \tag{7}$$

$$\begin{aligned}&\int_{S_q}\overline{e}_e^{d*}(\overline{x})\times\overline{H}(\overline{x})\cdot d\overline{a} \\ &\quad= \int_{S_\Sigma}\int_{S_q}\overline{J}(\overline{x}')\cdot\overline{\overline{K}}(\overline{x},\overline{x}')\cdot\overline{J}_e^{d*}(\overline{x})\,da\,da' \end{aligned} \tag{8}$$

where

$$\begin{aligned}\overline{\overline{K}}(\overline{x},\overline{x}') = &\int_{-\infty}^{\infty}\overline{h}_m^*(\zeta,\overline{x}')\overline{h}_m(\zeta,\overline{x})\,d\zeta \\ &+\int_{-\infty}^{\infty}\overline{h}_e^*(\zeta,\overline{x}')\overline{h}_e(\zeta,\overline{x})\,d\zeta \end{aligned} \tag{9}$$

and $\overline{J}_m^d(\overline{x}) = \hat{n}\times\overline{e}_m^d(\overline{x})$, $\overline{J}_e^d(\overline{x}) = \hat{n}\times\overline{e}_e^d(\overline{x})$ are modal equivalent currents. From these equations, the unknown coefficients are obtained.

III. Field Representation

Consider a perfectly conducting cylindrical waveguide with rectangular corrugations shown in Fig. 2 and assume an incident TE_{11} mode propagates in the input cylindrical waveguide. The waveguide medium permittivity and permeability are ε and μ. To simplify the field expressions, the field quantities are replaced by dimensionless ones and $e^{-i\omega t}$ is suppressed. This substitution is equivalent to replacing ε and μ with unity. With $e^{-i\omega t}$ time convention, the field is given by

$$\overline{E} = \sqrt{\mu}\,\overline{E}' \quad \overline{H} = -i\sqrt{\varepsilon}\,\overline{H}' \quad t = \sqrt{\mu\varepsilon}\,t'. \tag{10}$$

Maxwell's equations are then

$$\nabla\times\overline{E}' = i\frac{\partial\overline{H}'}{\partial t'} \quad \nabla\times\overline{H}' = i\frac{\partial\overline{E}'}{\partial t'}. \tag{11}$$

The fields can be represented by Hertz potentials such that

$$\overline{E}' = \nabla\times\nabla\times\overline{\Pi}_m + \omega\nabla\times\overline{\Pi}_e = \overline{E}_m + \overline{E}_e \tag{12}$$

$$\overline{H}' = \nabla\times\nabla\times\overline{\Pi}_e + \omega\nabla\times\overline{\Pi}_m = \overline{H}_e + \overline{H}_m \tag{13}$$

where $\overline{\Pi}_e$, $\overline{\Pi}_m$ are the electric and magnetic Hertz potentials, respectively.

In region I ($r < a$), the scattered field is represented by the Hertz potentials

$$\overline{\Pi}_m^s = \hat{z}\cos\phi\int_{-\infty}^{\infty}\tilde{\Pi}_m(\zeta)J_1(\kappa r)e^{i\zeta z}\,d\zeta \tag{14}$$

$$\overline{\Pi}_e^s = \hat{z}\sin\phi\int_{-\infty}^{\infty}\tilde{\Pi}_e(\zeta)J_1(\kappa r)e^{i\zeta z}\,d\zeta \tag{15}$$

where $\kappa = \sqrt{\omega^2-\zeta^2}$.

In region II ($r > a$, the corrugation region), the fields in the lth groove are expanded as a sum of discrete mode functions in terms of the Hertz vectors

$$\overline{\Pi}_m^d = \hat{z}\sum_{n=0}^{\infty}E_{nl}P_{nl}(\kappa_n r)\cos\phi\cos\frac{n\pi}{d}(z-s_l) \tag{16}$$

$$\overline{\Pi}_e^d = \hat{z}\sum_{n=1}^{\infty}H_{nl}Q_{nl}(\kappa_n r)\sin\phi\sin\frac{n\pi}{d}(z-s_l) \tag{17}$$

where

$$P_{nl}(\kappa_n r) = J_1(\kappa_n r)N_1(\kappa_n b_l) - J_1(\kappa_n b_l)N_1(\kappa_n r) \tag{18}$$

$$Q_{nl}(\kappa_n r) = J_1(\kappa_n r)N_1'(\kappa_n b_l) - J_1'(\kappa_n b_l)N_1(\kappa_n r) \tag{19}$$

and $\kappa_n = \sqrt{\omega^2-(n\pi/d)^2}$.

The incident field is represented as

$$\overline{\Pi}_e^i = \hat{z}J_1(\beta_c r)\sin\phi e^{i\beta z} \tag{20}$$

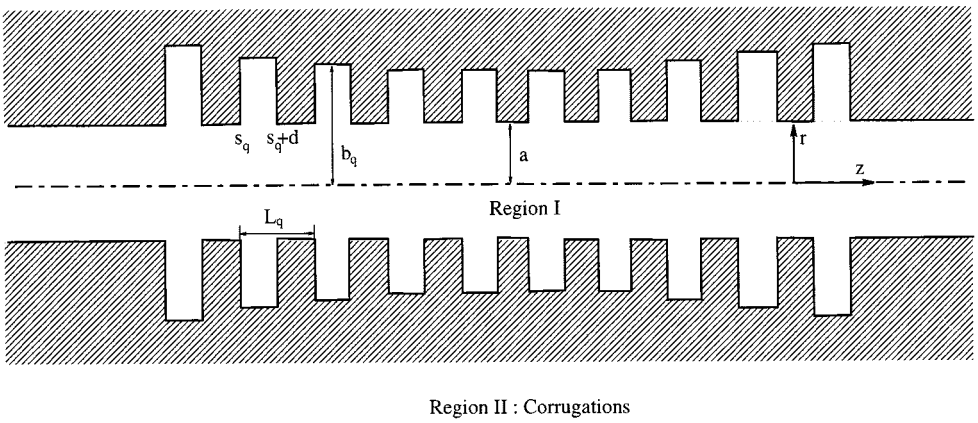

Fig. 2. Geometry of the problem.

where $\beta = \sqrt{\omega^2 - \beta_c^2}$, $\beta_c = \chi_1'/a$, and χ_1' is defined as the first root of the derivative of the first-order Bessel function $J_1(x)$, and $\hat{r}$, $\hat{\phi}$, and $\hat{z}$ denote unit vectors in cylindrical coordinates.

To obtain the simultaneous equations for the unknown coefficients E_{lm} and H_{lm}, we substitute (14)–(17) and (20), into (7) and (8)

$$\begin{aligned}
&\beta_c^2 J_1(\beta_c a) e^{i\beta s_l} \left(\frac{m\pi}{d}\right) F_m(-\beta) \\
&\quad - \sum_{n,l} E_{nl} \frac{P_{nl}(\kappa_n a)}{\omega a} \left[\left(\frac{n\pi}{d}\right)^2 I^{(2)} - \kappa_n^2 I^{(1)}\right] \frac{m\pi}{d} \\
&\quad + \sum_{n,l} H_{nl} \kappa_n Q_{nl}'(\kappa_n a) \frac{nm\pi^2}{d^2} I^{(2)} \\
&\quad = H_{mq} Q_{mq}(\kappa_m a) \kappa_m^2 \frac{d}{2}(1 - \delta_{m0}) \qquad (21)
\end{aligned}$$

$$\begin{aligned}
&\frac{\beta^2}{a} J_1(\beta_c a) e^{i\beta s_q} F_m(-\beta) + \sum_{n,l} H_{nl} \frac{n\pi\kappa_n}{ad} Q_{nl}'(\kappa_n a) I^{(1)} \\
&\quad - \sum_{n,l} E_{nl} \frac{P_{nl}(\kappa_n a)}{a^2 \omega} \left[\left(\frac{n\pi}{d}\right)^2 I^{(1)} - \kappa_n^2 I^{(3)} \right. \\
&\qquad \left. + (\omega\kappa_n a)^2 I^{(4)}\right] \\
&\quad = \left[H_{mq} \frac{m\pi}{d} \frac{Q_{mq}(\kappa_m a)}{a} - E_{mq} \kappa_m \omega P_{mq}'(\kappa_m a)\right] \\
&\qquad \cdot \frac{d}{2}(1 + \delta_{m0}) \qquad (22)
\end{aligned}$$

where

$$I^{(1)} = \frac{1}{2\pi} \int_{-\infty}^{\infty} \frac{\zeta^2 J_1(\kappa a)}{\kappa J_1'(\kappa a)} e^{i\zeta(s_q - s_l)} F_m(-\zeta) F_n(\zeta)\, d\zeta \qquad (23)$$

$$I^{(2)} = \frac{1}{2\pi} \int_{-\infty}^{\infty} \frac{\kappa J_1(\kappa a)}{J_1'(\kappa a)} e^{i\zeta(s_q - s_l)} F_m(-\zeta) F_n(\zeta)\, d\zeta \qquad (24)$$

$$I^{(3)} = \frac{1}{2\pi} \int_{-\infty}^{\infty} \frac{\zeta^4 J_1(\kappa a)}{\kappa^3 J_1'(\kappa a)} e^{i\zeta(s_q - s_l)} F_m(-\zeta) F_n(\zeta)\, d\zeta \qquad (25)$$

$$I^{(4)} = \frac{1}{2\pi} \int_{-\infty}^{\infty} \frac{\zeta^2 J_1'(\kappa a)}{\kappa J_1(\kappa a)} e^{i\zeta(s_q - s_l)} F_m(-\zeta) F_n(\zeta)\, d\zeta \qquad (26)$$

and

$$F_n(\zeta) = \frac{\left[1 - (-1)^n e^{-i\zeta d}\right]}{-\zeta^2 + \left(\frac{n\pi}{d}\right)^2}. \qquad (27)$$

It is possible to evaluate the integrals $I^{(1)}$, $I^{(2)}$, $I^{(3)}$, and $I^{(4)}$ as a fast-convergent series using a contour integration method [7], which leads to a calculation of pole contributions. The integrals contain poles due to Bessel functions and those due to F_m and F_n when $m = n$ and $q = l$. The result is

$$\begin{aligned}
I^{(1)} = &-i \sum_j \frac{\zeta_j' J_1(\chi_j')}{a J_1''(\chi_j')} A(q, l, m, n, \zeta_j') + \delta_{ql}\delta_{mn} \\
&\cdot (1 + 3\delta_{m0}) \frac{dJ_1(\kappa_m a)}{2\kappa_m J_1'(\kappa_m a)} \qquad (28)
\end{aligned}$$

$$\begin{aligned}
I^{(2)} = &-i \sum_j \frac{\chi_j'^2 J_1(\chi_j')}{a^3 \zeta_j' J_1''(\chi_j')} A(q, l, m, n, \zeta_j') + \delta_{ql}\delta_{mn} \\
&\cdot \frac{\kappa_m J_1(\kappa_m a)}{J_1'(\kappa_m a)} \frac{d^3}{(2m^2\pi^2 - 3\delta_{m0})} \qquad (29)
\end{aligned}$$

$$\begin{aligned}
I^{(3)} = &-i \sum_j \frac{a\zeta_j'^3 J_1(\chi_j')}{\chi_j'^2 J_1''(\chi_j')} A(q, l, m, n, \zeta_j') \\
&+ \delta_{ql}\delta_{mn} \frac{(m\pi)^2 J_1(\kappa_m a)}{2d\kappa_m^3 J_1'(\kappa_m a)} - i\frac{\omega^3 a}{2} A(q, l, m, n, \omega) \qquad (30)
\end{aligned}$$

$$\begin{aligned}
I^{(4)} = &-i \sum_j \frac{\zeta_j}{a} A(q, l, m, n, \zeta_j) + \delta_{ql}\delta_{mn} \\
&\cdot (1 + 3\delta_{m0}) \frac{dJ_1'(\kappa_m a)}{2\kappa_m J_1(\kappa_m a)} - i\frac{\omega}{2a} A(q, l, m, n, \omega) \qquad (31)
\end{aligned}$$

where

$$\begin{aligned}
A(q, l, m, n, \zeta) = &\frac{[1 + (-1)^{m+n}] e^{i\zeta|s_q - s_l|}}{\left[\zeta^2 - \left(\frac{m\pi}{d}\right)^2\right]\left[\zeta^2 - \left(\frac{n\pi}{d}\right)^2\right]} \\
&- \frac{(-1)^n e^{i\zeta|s_q - s_l - d|} + (-1)^m e^{i\zeta|s_q - s_l + d|}}{\left[\zeta^2 - \left(\frac{m\pi}{d}\right)^2\right]\left[\zeta^2 - \left(\frac{n\pi}{d}\right)^2\right]} \qquad (32)
\end{aligned}$$

and $\zeta_j = \sqrt{\omega^2 - (\chi_j/a)^2}$, $\zeta_j' = \sqrt{\omega^2 - (\chi_j'/a)^2}$, and χ_j, χ_j' are the jth root of $J_1(x)$, $J_1'(x)$, respectively.

Equations (21) and (22) constitute a set of simultaneous equations for the unknowns E_{nl} and H_{nl}. It is simple to solve these equations since the coefficients are calculated from a

rapidly convergent series and, thus, numerically efficient. To achieve numerical convergence, the number of modes in each corrugation, i.e., n, used in the calculation must at least satisfy $n > \omega d/\pi$. In the following numerical computations, $n = 2$ is enough for the accuracy to be 0.1%.

IV. Reflection and Transmission Coefficients

It is necessary to evaluate the transmitted and reflected powers as $z \to \pm\infty$. Using the residue calculus, we evaluate the scattered E-fields when $z \to \pm\infty$ as

$$\overline{E}' = \sum_j C_j^e \overline{e}_e^j e^{\pm i\zeta_j' z} + \sum_j C_j^m \overline{e}_m^j e^{\pm i\zeta_j z} \tag{33}$$

where

$$\overline{e}_m^j = \hat{r}\,\frac{i\zeta_j\chi_j}{a} J_1'\left(\frac{\chi_j r}{a}\right)\cos\phi - \hat{\phi}\,\frac{i\zeta_j}{r} J_1\left(\frac{\chi_j r}{a}\right)\sin\phi \pm \hat{z}\left(\frac{\chi_j}{a}\right)^2 J_1\left(\frac{\chi_j r}{a}\right)\cos\phi \tag{34}$$

$$\overline{e}_e^j = \hat{r}\,\frac{\omega}{r} J_1\left(\frac{\chi_j' r}{a}\right)\cos\phi - \hat{\phi}\,\frac{\omega\chi_j}{a} J_1'\left(\frac{\chi_j' r}{a}\right)\sin\phi \tag{35}$$

$$C_j^m = \frac{1}{\chi_j J_1'(\chi_j)} \sum_{n,l} E_{nl} P_{nl}(\kappa_n a)\kappa_n^2 B_{\pm}(\zeta_j, n, l) \tag{36}$$

$$C_j^e = \frac{i\omega}{\zeta_j'\chi_j'^2 J_1''(\chi_j')} \sum_{n,l} \left[D_1(j, n, l)E_{nl} + D_2(j, n, l)H_{nl}\right] \times B_{\pm}(\zeta_j', n, l) \tag{37}$$

where

$$D_1(j, n, l) = \left[\left(\frac{\chi_j'}{a}\right)^2 - \kappa_n^2\right] P_{nl}(\kappa_n a) \tag{38}$$

$$D_2(j, n, l) = -\frac{\kappa_n n\pi\chi_j'^2}{ad\omega} Q_{nl}'(\kappa_n a) \tag{39}$$

$$B_{\pm}(\xi, n, l) = \frac{e^{\mp i\xi s_l}\left[1 - (-1)^n e^{\mp i\xi d}\right]}{-\xi^2 + \left(\frac{n\pi}{d}\right)^2}. \tag{40}$$

The reflected TE mode power as $z \to -\infty$ becomes

$$P_r^e = \frac{\pi}{2}\sum_{j=1}^{j_1} \left|C_j^e\right|^2 \omega\zeta_j'\left(\chi_j'^2 - 1\right) J_1^2\left(\chi_j'\right) \tag{41}$$

where j_1 is the largest number that satisfies the condition $\omega^2 - (\chi_j'/a)^2 > 0$. The reflected TM mode power as $z \to -\infty$ becomes

$$P_r^m = \frac{\pi}{2}\sum_{j=1}^{j_2} \left|C_j^m\right|^2 \omega\zeta_j\chi_j^2 J_1'^2\left(\chi_j\right) \tag{42}$$

where j_2 is the largest number that satisfies the condition $\omega^2 - (\chi_j/a)^2 > 0$. The reflection coefficient $\rho = (P_r^e + P_r^m)/P_i$, where the incident power is given by

$$P_i = \frac{\pi}{2}\omega\zeta_1'\left(\chi_1'^2 - 1\right) J_1^2(\chi_1'). \tag{43}$$

In Fig. 3, we show the calculated return loss of a finite length corrugated waveguide connected with smooth-walled circular cylinders at both sides, as shown in Fig. 2. To check the validity of our method, we compared our results with those of the scattering matrix formulation in [4], thus confirming an agreement between them. While 10–15 modes in each cylinder section are needed in the calculation based on the scattering matrix formulation [4], our results are obtained with sufficient accuracy using two to three modes in each corrugation. This means that our computational scheme is five times more efficient than the one in [4].

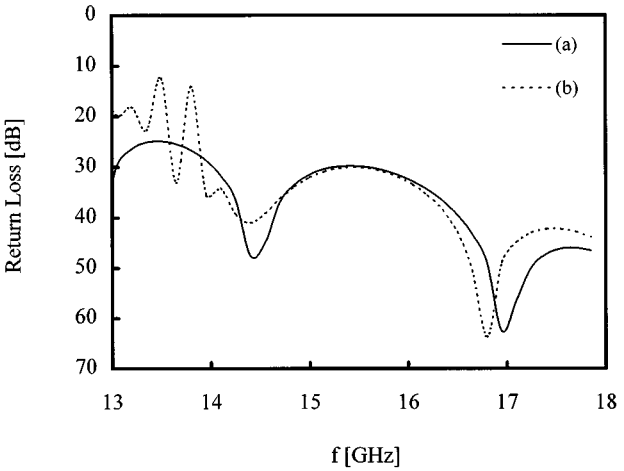

Fig. 3. Return loss of a cylindrical waveguide with a finite-length corrugated waveguide section. (a) Return loss calculated by the method presented in this paper. (b) Theoretical calculation based on the method in [4]. The waveguide dimensions are those of [4, Table I, case i)].

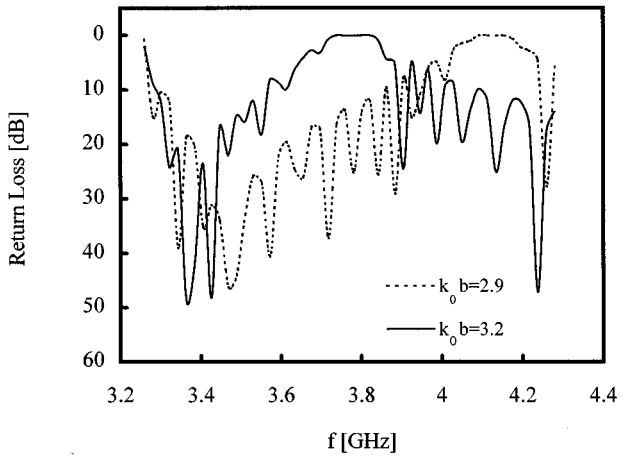

Fig. 4. Frequency characteristics of return loss of a corrugated waveguide section. The passband width becomes narrower as the outer radius b increases slightly. As shown in the figure, the 10-dB bandwidth in the figure changes from 600 to 300 MHz as the length increases ($k_0 a = 1.922$, $k_0 d = 0.7121$, $k_0 L = 1.068$, where k_0 is the wavenumber at the center frequency and L is the corrugation pitch).

Figs. 4 and 5 illustrate the frequency characteristics of the finite-length corrugated waveguide section. In Fig. 5, we show the variations of the bandwidth as the corrugation depth b changes. As the length of the radial waveguide (or, equivalently, the transmission line) changes slightly, the passband width changes appreciably. For instance, the 10-dB bandwidth changes from 600 to 300 MHz, as $k_0 b$ changes from 2.9 to 3.2 ($f_0 = 3.4$ GHz).

Fig. 5 shows the frequency responses of the return loss when $k_0 b$ changes from 2.5 to 5.5. It is seen that the curve shapes

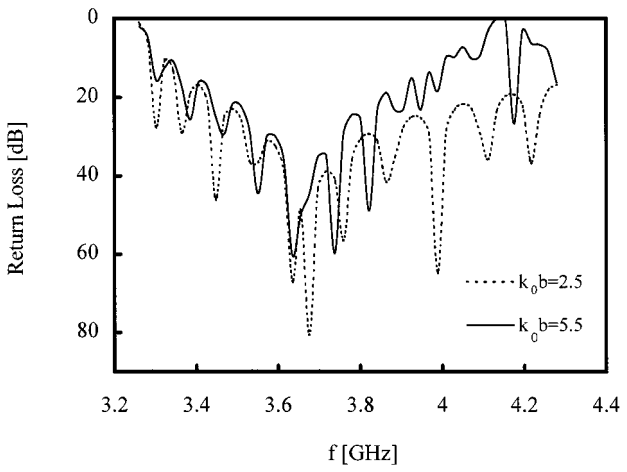

Fig. 5. Frequency characteristics of the return loss exhibits a periodic frequency response as the inner radius b increases ($k_0 a = 1.922$, $k_0 d = 0.7121$, $k_0 L = 1.068$, where k_0 is the wavenumber at the center frequency and L is the corrugation pitch).

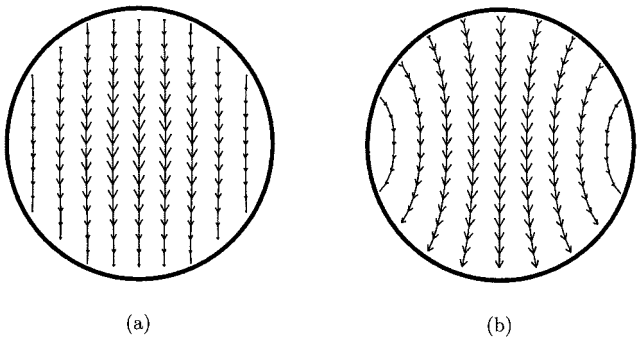

Fig. 6. Electric-field lines of the HE_{11} mode and the TE_{11} mode in the waveguide. (a) Field lines in the corrugated region. (b) Field lines far away from the corrugated region ($ka = 4.3358$, $kb = 6.1139$, $kd = 2.0823$, $kL = 3.9087$.)

change little, particularly in the low-frequency regime, where $f < 3.8$ GHz. This can be conjectured with the first-order approximation based on the transmission-line theory where a periodic frequency response is expected as $(b - a)$ is changed by a half-wavelength.

Our additional computations reveal that the return-loss variations with d and L are negligible, and when the number of corrugations increases, the number of ripples in the return-loss curve increases, as expected.

In Fig. 6, we plot the transverse electric-field lines in the waveguide. In the corrugated section, the incident TE_{11} field is transformed into the hybrid HE_{11} mode. As shown in the figure, the field lines in the corrugated section are linear, which implies the symmetry between the electric and magnetic fields. In addition, the transverse electric field vanishes identically along the perimeter and results in the desirable characteristics of low attenuation. This can be guessed from the soft boundary conditions imposed by the corrugated surface when the corrugation depth is about $\lambda/4$ [8].

V. Conclusion

A rapidly converging series solution for scattering from a cylindrical waveguide with rectangular corrugations have been obtained. Numerical computations have been performed to illustrate the scattering behavior of a number of waveguide sections. The comparison to other existing data shows an agreement. Our series solution is analytic and in closed form, thus, it is numerically efficient and simple to use.

Appendix
Infinite Corrugated Waveguide

When the number of corrugations is increased to infinity, the mode coefficients E_{nl} and H_{nl} in (16) and (17) are reduced to $e^{i\beta lL}E_n$, $e^{i\beta lL}H_n$, where L is the corrugation pitch. That is, modal currents in a corrugation is related to those in another corrugation by $e^{i\beta L}$, which is based on Floquet's theorem. The propagation constant β is yet an unknown constant, but can be found from (21) and (22).

With the substitutions above, (21) and (22) are the same, except that a factor is added to the integrands in $I^{(1)}$, $I^{(2)}$, $I^{(3)}$, and $I^{(4)}$, and the incident field is omitted. Hence,

$$\begin{aligned}
&-\sum_n E_n \frac{P_n(\kappa_n a)}{\omega a}\left[\left(\frac{n\pi}{d}\right)^2 I^{(2)} - \kappa_n^2 I^{(1)}\right]\frac{m\pi}{d} \\
&\quad + \sum_n H_n \kappa_n Q_n'(\kappa_n a)\frac{nm\pi^2}{d^2} I^{(2)} \\
&\quad = H_m Q_m(\kappa_m a)\kappa_m^2 \frac{d}{2}(1-\delta_{m0}) \qquad (44)\\
&\sum_n H_n \frac{n\pi\kappa_n}{ad} Q_n'(\kappa_n a) I^{(1)} \\
&\quad - \sum_n E_n \frac{P_n(\kappa_n a)}{a^2\omega}\left[\left(\frac{n\pi}{d}\right)^2 I^{(1)} - \kappa_n^2 I^{(3)}\right. \\
&\qquad\qquad \left. + (\omega\kappa_n a)^2 I^{(4)}\right] \\
&\quad = \left[H_m \frac{m\pi}{d}\frac{Q_m(\kappa_m a)}{a} - E_m \kappa_m \omega P_m'(\kappa_m a)\right] \\
&\qquad \cdot \frac{d}{2}(1+\delta_{m0}) \qquad (45)
\end{aligned}$$

where

$$I^{(1)} = \frac{1}{2\pi}\int_{-\infty}^{\infty} \frac{\zeta^2 J_1(\kappa a)}{\kappa J_1'(\kappa a)} H(\beta,\zeta) F_m(-\zeta) F_n(\zeta)\, d\zeta \qquad (46)$$

$$I^{(2)} = \frac{1}{2\pi}\int_{-\infty}^{\infty} \frac{\kappa J_1(\kappa a)}{J_1'(\kappa a)} H(\beta,\zeta) F_m(-\zeta) F_n(\zeta)\, d\zeta \qquad (47)$$

$$I^{(3)} = \frac{1}{2\pi}\int_{-\infty}^{\infty} \frac{\zeta^4 J_1(\kappa a)}{\kappa^3 J_1'(\kappa a)} H(\beta,\zeta) F_m(-\zeta) F_n(\zeta)\, d\zeta \qquad (48)$$

$$I^{(4)} = \frac{1}{2\pi}\int_{-\infty}^{\infty} \frac{\zeta^2 J_1'(\kappa a)}{\kappa J_1(\kappa a)} H(\beta,\zeta) F_m(-\zeta) F_n(\zeta)\, d\zeta \qquad (49)$$

and

$$H(\beta,\zeta) = \lim_{N\to\infty} \frac{e^{-iNL(\beta-\zeta)} - e^{iNL(\beta-\zeta)}}{1 - e^{iL(\beta-\zeta)}}. \qquad (50)$$

The characteristic equations (44) and (45) are identical to those in [9] and confirm the validity of our approach.

REFERENCES

[1] A. J. Simmons and A. F. Kay, "The scalar feed-high performance feed for large paraboloid reflectors," in *IEE Conf. Pub.*, 1966, pp. 213–217.

[2] H. C. Minnett and B. M. Thomas, "A method of synthesizing radiation patterns with axial symmetry," *IEEE Trans. Antennas Propagat.*, vol. AP-14, pp. 654–656, Sept. 1966.

[3] P. J. B. Clarricoats and P. K. Saha, "Propagation and radiation behavior of corrugated feeds. I. Corrugated waveguide feed," *Proc. Inst. Elect. Eng.*, vol. 118, no. 3, pp. 1167–1176, 1971.

[4] G. L. James, "Analysis and design of TE_{11} to HE_{11} corrugated cylindrical waveguide mode converters," *IEEE Trans. Microwave Theory Tech.*, vol. 29, pp. 1059–1066, Oct. 1981.

[5] L. C. Da Silva, "A method of analysis of TE_{11} to HE_{11} mode converters," *IEEE Trans. Microwave Theory Tech.*, vol. 36, pp. 480–488, Mar. 1988.

[6] L. C. Da Silva and M. G. Castello Branco, "Analysis of the junction between smooth and corrugated cylindrical waveguides in mode converters," *IEEE Trans. Microwave Theory Tech.*, vol. 38, pp. 800–802, June 1990.

[7] G. Arfken, *Mathematical Methods for Physicists*. New York: Academic, 1995, pp. 427–429.

[8] P.-S. Kildal, "Artificially soft and hard surfaces in electromagnetics," *IEEE Trans. Microwave Theory Tech.*, vol. 38, pp. 1537–1544, Oct. 1990.

[9] I. G. Tigelis, J. L. Vomvoridis, and S. Tzima, "High frequency electromagnetic modes in a dielectric ring loaded beam tunnel," *IEEE Trans. Plasma Sci.*, vol. 26, pp. 922–930, June 1998.

Haeng S. Lee was born in Korea, in 1971. He received the B.S. degree in electronic engineering from the Seoul National University, Seoul, Korea, in 1995, and the M.S. and Ph.D. degrees in electrical engineering from the Korea Advanced Institute of Science and Technology, Taejon, Korea, in 1997 and 2000, respectively.

He is currently with the LCT Electronics Institute of Technology, Taejon, Korea, where his research interests include electromagnetic theory, scattering, and electromagnetic interference.

Hyo J. Eom (S'78–M'81–SM'99) received the B.S. degree in electronic engineering from the Seoul National University, Seoul, Korea, in 1973, and the M.S. and Ph.D. degrees in electrical engineering from the University of Kansas, Lawrence, in 1977 and 1982, respectively.

From 1981 to 1984, he was a Research Associate in the Remote Sensing Laboratory, University of Kansas. From 1984 to 1989, he was on the faculty of the Department of Electrical Engineering and Computer Science, University of Illinois, Chicago. In 1989, he joined the Department of Electrical Engineering, Korea Advanced Institute of Science and Technology, Taejon, Korea, where he is currently a Professor. His research interests are wave diffraction and scattering.